AMERICAN SOCIETY FOR MICROBIOLOGY | Molecular and Cellular Biology®

RESEARCH ARTICLE

CKS1 Germ Line Exclusion Is Essential for the Transition from Meiosis to Early Embryonic Development

Zdenka Ellederova,[a,b] Sonia del Rincon,[a,c] Marketa Koncicka,[d,e] Andrej Susor,[d] Michal Kubelka,[d] Dahui Sun,[a] Charles Spruck[a]

[a]Tumor Initiation and Maintenance Program, Sanford | Burnham | Prebys Medical Discovery Institute, La Jolla, California, USA
[b]Laboratory of Cell Regeneration and Plasticity, Institute of Animal Physiology and Genetics, Czech Academy of Science, Libechov, Czech Republic
[c]Gerald Bronfman Department of Oncology, McGill University Lady Davis Institute, Segal Cancer Centre-Jewish General Hospital, Montreal, Quebec, Canada
[d]Laboratory of Biochemistry and Molecular Biology of Germ Cells, Institute of Animal Physiology and Genetics, Czech Academy of Science, Libechov, Czech Republic
[e]Department of Cell Biology, Faculty of Science, Charles University, Prague, Czech Republic

ABSTRACT Cell division cycle (Cdc) kinase subunit (CKS) proteins bind cyclin-dependent kinases (CDKs) and play important roles in cell division control and development, though their precise molecular functions are not fully understood. Mammals express two closely related paralogs called CKS1 and CKS2, but only CKS2 is expressed in the germ line, indicating that it is solely responsible for regulating CDK functions in meiosis. Using *cks2*$^{-/-}$ knockout mice, we show that CKS2 is a crucial regulator of maturation-promoting factor (MPF; CDK1-cyclin A/B) activity in meiosis. *cks2*$^{-/-}$ oocytes display reduced and delayed MPF activity during meiotic progression, leading to defects in germinal vesicle breakdown (GVBD), anaphase-promoting complex/cyclosome (APC/C) activation, and meiotic spindle assembly. *cks2*$^{-/-}$ germ cells express significantly reduced levels of the MPF components CDK1 and cyclins A1/B1. Additionally, injection of MPF plus CKS2, but not MPF alone, restored normal GVBD in *cks2*$^{-/-}$ oocytes, demonstrating that GVBD is driven by a CKS2-dependent function of MPF. Moreover, we generated *cks2*$^{cks1/cks1}$ knock-in mice and found that CKS1 can compensate for CKS2 in meiosis *in vivo*, but homozygous embryos arrested development at the 2- to 5-cell stage. Collectively, our results show that CKS2 is a crucial regulator of MPF functions in meiosis and that its paralog, CKS1, must be excluded from the germ line for proper embryonic development.

KEYWORDS CKS, cyclin-dependent kinases, developmental biology, meiosis

Cell division cycle (Cdc) kinase subunit (CKS) proteins were originally identified through their ability to genetically suppress defective cyclin-dependent kinase (CDK) alleles in both fission (*Schizosaccharomyces pombe*) and budding (*Saccharomyces cerevisiae*) yeasts (1–3). Subsequent investigations demonstrated that these small (9- to 18-kDa), highly conserved proteins are ubiquitous in eukaryotes and physically interact with CDKs. Whereas lower eukaryotes express one CKS protein, humans, mice, and possibly other vertebrates express two CKS paralogs that are highly similar at the amino acid level (4).

Genetic and biochemical studies mostly in lower eukaryotes have shown that CKS proteins play important roles in mitosis (M phase), though other molecular functions have been suggested (5, 6). Genetic disruption of *cks1* in *S. pombe* leads to condensed but unsegregated chromosomes, an extended spindle structure, and elevated CDK1-cyclin B kinase activity, consistent with an M phase arrest (7). In *Xenopus*, the CKS ortholog Xe-p9 performs multiple essential functions in both M phase entry and the metaphase-to-anaphase transition (8).

In both mitotic and meiotic cell division cycles, M phase is regulated by maturation-

Citation Ellederova Z, del Rincon S, Koncicka M, Susor A, Kubelka M, Sun D, Spruck C. 2019. CKS1 germ line exclusion is essential for the transition from meiosis to early embryonic development. Mol Cell Biol 39:e00590-18. https://doi.org/10.1128/MCB.00590-18.

Copyright © 2019 American Society for Microbiology. All Rights Reserved.

Address correspondence to Charles Spruck, cspruck@sbpdiscovery.org.

Received 20 December 2018
Returned for modification 25 January 2019
Accepted 4 April 2019
Accepted manuscript posted online 15 April 2019
Published 13 June 2019

promoting factor (MPF), which is composed of CDK1, cyclin A/B, and CKS. However, the precise molecular function(s) of CKS proteins in regulating MPF activity remains unclear. CKS proteins have been proposed to function as adaptors that physically link CDK-cyclins to partially phosphorylated substrates for further phosphorylation (9). For example, Xe-p9 promotes CDK1-dependent phosphorylation of CDC25, MYT1, and WEE1, leading to MPF activation (10), and MPF-mediated phosphorylation of the anaphase-promoting complex/cyclosome (APC/C) ubiquitin ligase, which is essential for M phase exit (11). In *S. cerevisiae*, CKS proteins also stimulate the transcription of APC/C regulator CDC20 by recruiting the 26S proteasome to the *cdc20* promoter (12).

Mouse knockout studies have demonstrated that CKS1/2 perform both redundant and specialized roles in cell division control and development. *cks1*$^{-/-}$ mice are viable and fertile; however, adult mice are ~25% smaller than their wild-type (wt) littermates (13). *cks1*$^{-/-}$ mouse embryo fibroblasts (MEFs) also grow poorly in culture and senesce prematurely. These physiological and cellular defects were attributed to a paralog-specific function of CKS1 as an essential cofactor of the SCF^{SKP2} ubiquitin ligase, which promotes the ubiquitin-dependent proteolysis of several CDK inhibitors, including p27^{KIP1}, p21^{CIP1}, p57^{KIP2}, and p130 (13, 14). In contrast, *cks2*$^{-/-}$ knockout mice are sterile for both sexes, with germ cells failing to progress past metaphase of meiosis division I (MI) (15). Interestingly, CKS2 is the only CKS paralog that is expressed in oocytes and spermatocytes, though microinjection of either *cks1* or *cks2* mRNA into *cks2*$^{-/-}$ oocytes was shown to be sufficient to rescue the metaphase I arrest (15). Therefore, it is unclear as to why CKS2 is solely responsible for regulating CDK functions in meiosis. *cks1*$^{-/-}$ *cks2*$^{-/-}$ double-knockout (DKO) mice die early in embryogenesis at or before the morula stage (before embryonic day 3.5 [<E3.5]), indicating an essential role for CKS proteins in mammalian development (16).

In the present study, we sought to define the role of CKS2 in regulating MPF functions in meiosis and determine why CKS2 is the sole CKS paralog expressed in the germ line. Our study demonstrates that *cks2*$^{-/-}$ oocytes exhibit reduced/delayed MPF activity that is attributed to reduced MPF component expression, leading to defects in germinal vesicle breakdown (GVBD), APC/C activation, and meiotic spindle assembly. Furthermore, we generated *cks2*$^{cks1/cks1}$ knock-in (KI) mice and found that CKS1 can compensate for CKS2 in meiosis *in vivo*, but its expression in the germ line causes the arrest of embryonic development at the 2- to 5-cell stage.

RESULTS

***cks2*$^{-/-}$ oocytes exhibit delayed GVBD and reduced MPF/MAPK kinase activities.** CKS2 is required for progression through metaphase of meiosis division I (15). Therefore, we investigated whether upstream meiotic events might also be affected by CKS2 deficiency. Germinal vesicle (GV) stage oocytes isolated from *cks2*$^{-/-}$ mice displayed no obvious defects in maturation, including the presence of condensed chromatin, compared to wt oocytes (Fig. 1A). However, following the resumption of meiosis, *cks2*$^{-/-}$ oocytes demonstrated a significant delay in GVBD (Fig. 1B). Microscopic examination of the GVs revealed that GVBD was delayed approximately 2 h in the *cks2*$^{-/-}$ oocytes compared to the wt oocytes (wt oocytes, 1.05 h; *cks2*$^{-/-}$oocytes, 3.10 h; $P < 0.001$) (Fig. 1C). Next, we analyzed the timing and level of MPF kinase activity in *cks2*$^{-/-}$ oocytes following meiotic resumption using *in vitro* kinase assays with histone H1 as the substrate. Whereas wt oocytes exhibited detectable MPF activity within 2 h following the resumption of meiosis and maximal activity at approximately 4 h, MPF activity was detected in *cks2*$^{-/-}$ oocytes at 6 h, with maximal activity being seen at 8 h (Fig. 1D). In addition, MPF kinase activity in *cks2*$^{-/-}$ oocytes was reduced at all time points compared to that in wt oocytes (Fig. 1D). MPF activity was previously shown to induce expression of oocyte maturation factor MOS, which stimulates mitogen-activated protein kinase (MAPK) activity to promote meiotic spindle assembly (17). Consistent with this, *in vitro* kinase assays showed that MAPK activity was delayed (wt oocytes, 4 h; *cks2*$^{-/-}$oocytes, 6 h) and reduced at all time points in *cks2*$^{-/-}$ oocytes (Fig. 1D). Immunoblot analysis demonstrated that MAPK phosphorylation, a marker of

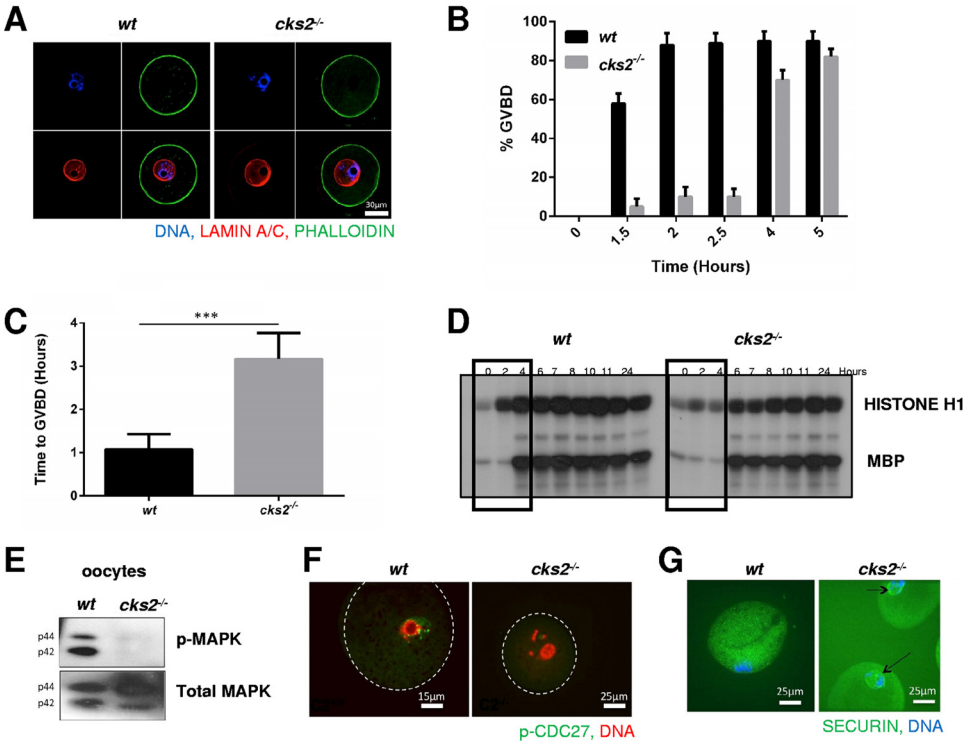

FIG 1 Delayed GVBD and delayed/reduced MPF/MAPK activities in *cks2*$^{-/-}$ oocytes. (A) GV stage *cks2*$^{-/-}$ oocytes display normal development. ICC analysis shows staining of DNA (DAPI; blue), cortical actin (green), and lamin A/C (red) in wt and *cks2*$^{-/-}$ GV stage oocytes. (B) Delayed GVBD in *cks2*$^{-/-}$ oocytes. (C) Graphical representation of the data presented in panel B. The timing of GVBD was 1.05 h for wt oocytes and 3.10 h for *cks2*$^{-/-}$ oocytes. A total of ≥18 oocytes were analyzed. Data represent the mean ± SD. ***, $P < 0.001$, Student's *t* test. (D) MPF and MAPK kinase activities are delayed and reduced in *cks2*$^{-/-}$ oocytes. GV stage oocytes were stimulated to resume meiosis and harvested at the indicated times, and extracts were subjected to *in vitro* kinase assays using histone H1 (MPF) and MBP (MAPK) as the substrates. (E) Immunoblots showing reduced phosphorylated MAPK (p-MAPK), a marker of activation, in *cks2*$^{-/-}$ oocytes, at 3 h post-meiotic resumption. (F) ICC analysis showing the absence of phosphorylation of APC/C component CDC27 in *cks2*$^{-/-}$ oocytes at 7 h post-meiotic resumption. (G) ICC analysis demonstrating the persistence of securin in *cks2*$^{-/-}$ oocytes at 8 h post-meiotic resumption.

its activation, was absent in *cks2*$^{-/-}$ oocytes at 3 h post-meiotic resumption (Fig. 1E). We then analyzed *cks2*$^{-/-}$ oocytes for defects in MPF-dependent downstream processes during meiotic maturation. One target of MPF kinase activity is CDC27, which activates APC/C ubiquitin ligase activity, leading to the degradation of securin and the stimulation of chromatid segregation (18, 19). Immunocytochemical (ICC) analysis demonstrated that CDC27 phosphorylation was absent and securin persisted at 8 h post-meiotic resumption in *cks2*$^{-/-}$ oocytes, consistent with a defect in MPF activation (Fig. 1F and G). Collectively, these data demonstrate that *cks2*$^{-/-}$ oocytes exhibit delayed GVBD, likely attributed to delayed and/or reduced MPF/MAPK kinase activities.

***cks2*$^{-/-}$ germ cells display reduced expression of CDK1 and cyclins A and B1.** To investigate the underlying mechanism(s) for the reduced MPF activity in *cks2*$^{-/-}$ oocytes, we analyzed the expression of MPF components and regulatory factors by quantitative reverse transcription-PCR (qRT-PCR). GV stage *cks2*$^{-/-}$ oocytes were found to contain significantly reduced levels of *cdk1*, *ccnb1* (cyclin B1), and *ccna1* (cyclin A1) compared to stage-matched wt oocytes (Fig. 2A). The levels of *cdk2* and *cdc20* were also reduced in *cks2*$^{-/-}$ oocytes. Moreover, *cdk1* expression was found to be reduced in *cks2*$^{-/-}$ spermatocytes and MEFs (Fig. 2B). Of note, the reduced *cdk1* expression in *cks2*$^{-/-}$ MEFs could be rescued by the transduction of cells with CKS2-expressing retroviruses, confirming that the defect was caused by the absence of CKS2 (Fig. 2B). The reduced amount of CDK1 in *cks2*$^{-/-}$ oocytes and spermatocytes was further confirmed by immunoblotting (Fig. 2C and D). Furthermore, we found that *cks2*$^{-/-}$ oocytes contained increased inhibitory phosphorylation of CDK1 at tyrosine 15 (Tyr15),

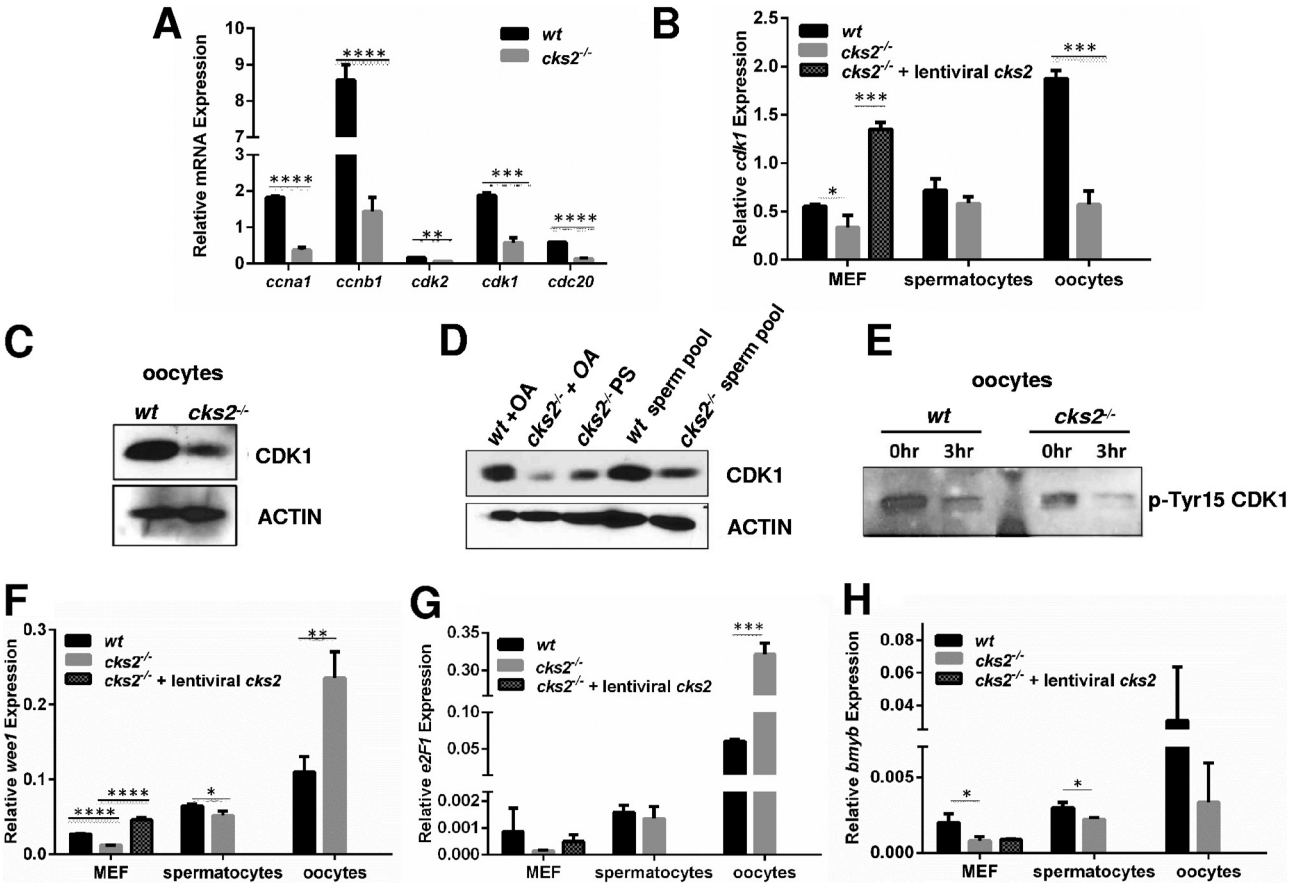

FIG 2 Reduced expression of MPF components *cdk1*, *ccna1*, and *ccnb1* in *cks2*$^{-/-}$ oocytes. (A) qRT-PCR analysis showing reduced expression of MPF components in *cks2*$^{-/-}$ oocytes. Expression of *cdk2* and *cdc20* is also shown. Data represent the mean ± SD. Significance was determined by Student's *t* test. ****, $P < 0.0001$; ***, $P < 0.001$; **, $P < 0.01$. (B) Reduced *cdk1* expression in *cks2*$^{-/-}$ oocytes, spermatocytes, and MEFs. Expression of *cks2* in *cks2*$^{-/-}$ MEFs restored the expression of *cdk1* to the wt level. Data represent the mean ± SD. Significance was determined by Student's *t* test. ***, $P < 0.001$; *, $P < 0.05$. (C) Immunoblots confirming reduced CDK1 in *cks2*$^{-/-}$ oocytes. Actin is shown as a loading control. (D) Immunoblots showing reduced CDK1 in *cks2*$^{-/-}$ spermatocytes. (E) Immunoblot of phosphorylated-Tyr15 (p-Tyr15) CDK1 in wt and *cks2*$^{-/-}$ oocytes. GV stage oocytes were analyzed at 3 h post-meiotic resumption. Normalized p-Tyr15 CDK1 is 1:1.40 wt/*cks2*$^{-/-}$. (F to H) qRT-PCR analysis of *wee1* (F), *e2f1* (G), and *bmyb* (H) in wt and *cks2*$^{-/-}$ oocytes, spermatocytes, and MEFs. *wee1* and *e2f1* expression was restored in *cks2*$^{-/-}$ MEFs by enforced *cks2* expression. Data represent the mean ± SD. Significance was determined by Student's *t* test. ****, $P < 0.0001$; ***, $P < 0.001$; **, $P < 0.01$; *, $P < 0.05$.

which, when normalized to total CDK1 levels, represented an approximately 40% increase compared to that in wt oocytes (Fig. 2C and E). To explore the potential cause(s) of the reduced CDK1 expression/activity in *cks2*$^{-/-}$ oocytes, we analyzed the expression of CDK1-activating kinase gene *wee1* and genes for its transcriptional regulators, *e2F1* and *bmyb*, by qRT-PCR. Whereas expression of *wee1*, *e2F1*, and *bmyb* was reduced in *cks2*$^{-/-}$ MEFs and spermatocytes, expression of *wee1* and *e2F1* was significantly increased in *cks2*$^{-/-}$ oocytes (Fig. 2F to H). Furthermore, retrovirus-mediated expression of CKS2 in *cks2*$^{-/-}$ MEFs restored the expression of *wee1* and *e2F1* to a level comparable to that in wt MEFs (Fig. 2F and G). These results suggest that the reduced and delayed MPF activity observed in *cks2*$^{-/-}$ germ cells is likely attributed to decreased *cdk1* expression and dysregulation of CDK1 activation and that CDK1 expression in oocytes may be differentially regulated compared to other cell types.

***cks2*$^{-/-}$ oocytes display defective MI spindle assembly.** MPF and MAPK play crucial roles in regulating meiotic spindle assembly (20). Since *cks2*$^{-/-}$ oocytes exhibited delayed and reduced MPF and MAPK kinase activities, we next determined whether these cells were also defective in MI spindle assembly. As expected, ICC analysis of microtubules showed that normal spindles formed in wt oocytes arrested at metaphase I (Fig. 3A). In contrast, *cks2*$^{-/-}$ oocytes displayed defective spindles, with chromosomes failing to align on the metaphase plate (Fig. 3A). Moreover, *cks2*$^{-/-}$

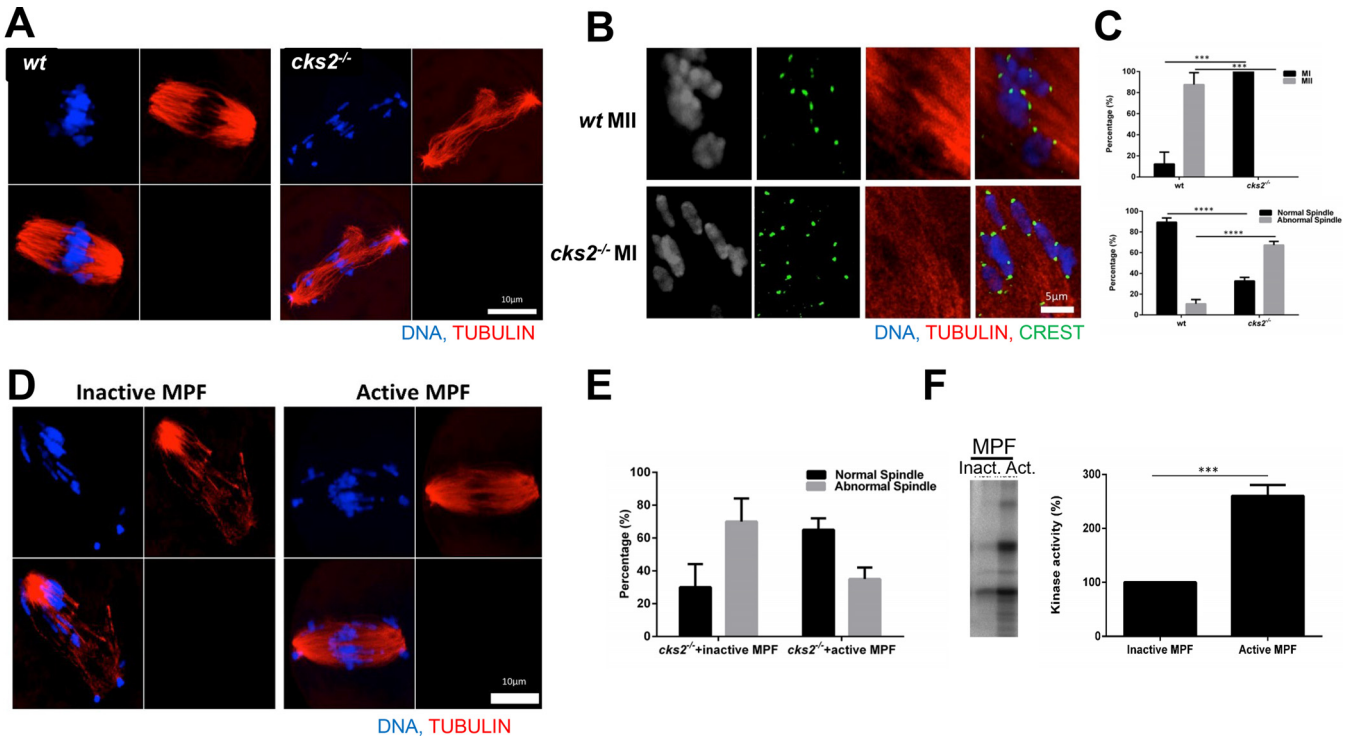

FIG 3 Aberrant MI spindle assembly in *cks2*$^{-/-}$ oocytes can be rescued by MPF. (A) ICC images showing aberrant MI spindles in *cks2*$^{-/-}$ oocytes, as indicated by tubulin (red) and DNA (DAPI; blue) staining. (B) Absence of appropriately resolved chiasmata in *cks2*$^{-/-}$ oocytes. The ICC image shows tubulin (red), DNA (blue), and kinetochores (crest antibody; green). (C) Quantification of the meiotic phenotype and spindle morphology. (D) Microinjection of active MPF into *cks2*$^{-/-}$ oocytes rescues the MI spindle defect. (E) Quantification of the spindle morphology after injection of active MPF. (F) *In vitro* kinase assays confirming the activities of microinjected MPF samples. Data represent the mean ± SD. Significance was determined by Student's *t* test. ****, $P < 0.0001$; ***, $P < 0.001$.

oocytes that arrested in metaphase of MI exhibited nonseparated chromosomes, suggesting a failure to properly resolve chiasmata (Fig. 3B). To determine whether the spindle assembly defect in *cks2*$^{-/-}$ oocytes was caused by reduced MPF activity, we microinjected inactive or active MPF into *cks2*$^{-/-}$ oocytes and examined MI spindle assembly by ICC. Whereas microinjection of inactive MPF could not rescue the MI spindle assembly defect, *cks2*$^{-/-}$ oocytes microinjected with active MPF displayed partially rescued spindles (Fig. 3C). We confirmed the inactive and active status of the microinjected MPF by *in vitro* kinase assays (Fig. 3D). These results demonstrate that the MI spindle assembly defect in *cks2*$^{-/-}$ oocytes is likely caused by reduced MPF activity.

Microinjection of active MPF plus CKS2 rescues the GVBD delay in *cks2*$^{-/-}$ oocytes. We next sought to determine the molecular cause(s) of the GVBD delay in *cks2*$^{-/-}$ oocytes. GV stage oocytes from *cks2*$^{-/-}$ mice were microinjected with various MPF components, and the ability to rescue the GVBD delay was assessed by microscopic evaluation. As expected, *cks2*$^{-/-}$ oocytes microinjected with inactive MPF demonstrated delayed GVBD comparable to that in noninjected *cks2*$^{-/-}$ oocytes (Fig. 4). In contrast, microinjection of active MPF or recombinant CKS2 protein alone into *cks2*$^{-/-}$ oocytes reduced the GVBD delay by nearly 1 h. However, microinjection of active MPF plus CKS2 protein completely rescued the GVBD delay, comparable to the timing in noninjected wt oocytes. Interestingly, we found that microinjection of recombinant CKS1 protein into *cks2*$^{-/-}$ oocytes rescued the GVBD delay more effectively than microinjection of CKS2 protein and that the delay was nearly comparable to that in *cks2*$^{-/-}$ oocytes microinjected with active MPF plus CKS2 protein. These results demonstrate that CKS2-dependent MPF functions mediate GVBD in mammalian oocytes.

CKS1 can compensate for CKS2 in mammalian meiosis but is deleterious for early embryonic development. Previously, it was shown that microinjection of *cks1*

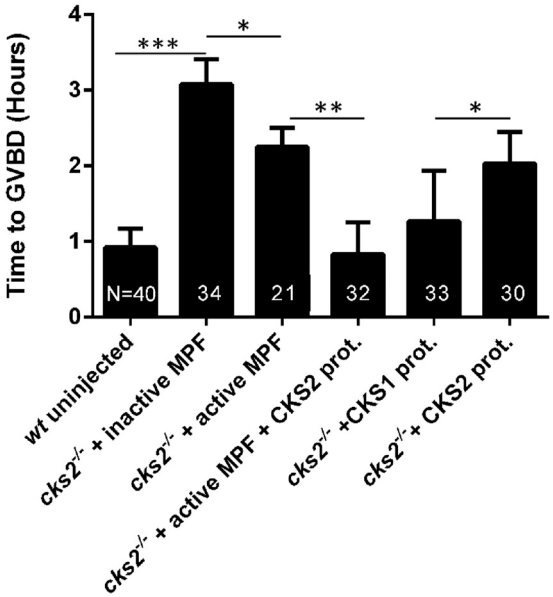

FIG 4 Microinjection of MPF plus CKS2 or CKS1 alone rescues the GVBD delay in *cks2*$^{-/-}$ oocytes. Oocytes were injected with the indicated proteins. and the timing of GVBD was assessed by microscopic examination. Data represent the mean ± SD. Significance was determined by Student's *t* test. *, $P < 0.05$; **, $P < 0.01$; ***, $P < 0.001$.

mRNA into *cks2*$^{-/-}$ oocytes could rescue the metaphase I arrest (15). Additionally, our data presented above show that microinjection of CKS1 protein into *cks2*$^{-/-}$ oocytes rescues the GVBD delay more effectively than microinjection of CKS2 (Fig. 4). It is therefore perplexing as to why CKS1 is excluded from the germ line if it can compensate for CKS2 functions in meiosis *in vitro*. To address this question, we generated knock-in (KI) mice that express *cks1* from the endogenous *cks2* promoter by homologous recombination (designated *cks2*$^{cks1/cks1}$ mice) (Fig. 5A). Heterozygous *cks2*$^{cks1/+}$ embryonic stem (ES) cells were injected into mouse blastocysts to generate chimeras, and germ line transmission was confirmed by PCR (Fig. 5B). *cks2*$^{cks1/+}$ mice were interbred and produced *cks2*$^{cks1/+}$ and *cks2*$^{+/+}$ mice at approximately the expected 2:1 ratio; however, no homozygous *cks2*$^{cks1/cks1}$ mice were detected out of 283 adult mice genotyped (Fig. 5C). We also failed to detect *cks2*$^{cks1/cks1}$ midgestation embryos between E7.5 and E13.5 from 83 embryos genotyped (Fig. 5C). These results suggest that *cks2*$^{cks1/cks1}$ mice are not viable. In support of this, *cks2*$^{cks1/+}$ intercrosses demonstrated a 25% frequency of embryo reabsorption *in utero*, compared to only 2% for wt intercrosses (Fig. 5D and E). We therefore examined *cks2*$^{cks1/+}$ intercrosses for blastocyst formation at E3.5. Whereas 69% of embryos from *cks2*$^{cks1/+}$ intercrosses matured to form normal blastocysts at E3.5, 15% arrested development at the 2-cell stage and 16% arrested at the 4- or 5-cell stage (Fig. 5F). By comparison, the frequency of 2- to 5-cell-stage E3.5 embryos from wt intercrosses was only 2% (data not shown). Genotyping of the 2- to 5-cell stage embryos from *cks2*$^{cks1/+}$ intercrosses revealed that they were homozygous for the *cks2*^{cks1} allele (Fig. 5G). In contrast, normal blastocysts isolated from the *cks2*$^{cks1/+}$ intercrosses were either the wt or *cks2*$^{cks1/+}$ genotype (Fig. 5G). These data demonstrate that CKS1 could compensate for CKS2 in meiosis and that *cks2*^{cks1} oocytes could be appropriately fertilized. *cks2*$^{cks1/cks1}$ mice are not viable, and *cks2*^{cks1} oocytes derived from *cks2*$^{cks1/+}$ mice are expected to contain abundant maternal transcripts that can overcome *cks2* deficiency (21), thus prohibiting the molecular analysis of *cks2*^{cks1} oocytes. We therefore analyzed MPF regulation in MEFs derived from *cks2*$^{cks1/+}$ embryos. *cks2*$^{cks1/+}$ MEFs contained reduced CDK1 expression and increased inhibitory pTyr15-CDK1 compared to wt MEFs (Fig. 5H). In addition, *cks2*$^{cks1/+}$ MEFs displayed increased CDK2 and reduced p27^{KIP1}, a substrate of SCF$^{SKP2\text{-}CKS1}$-mediated degradation. These results demonstrate that although CKS1 can compensate for CKS2

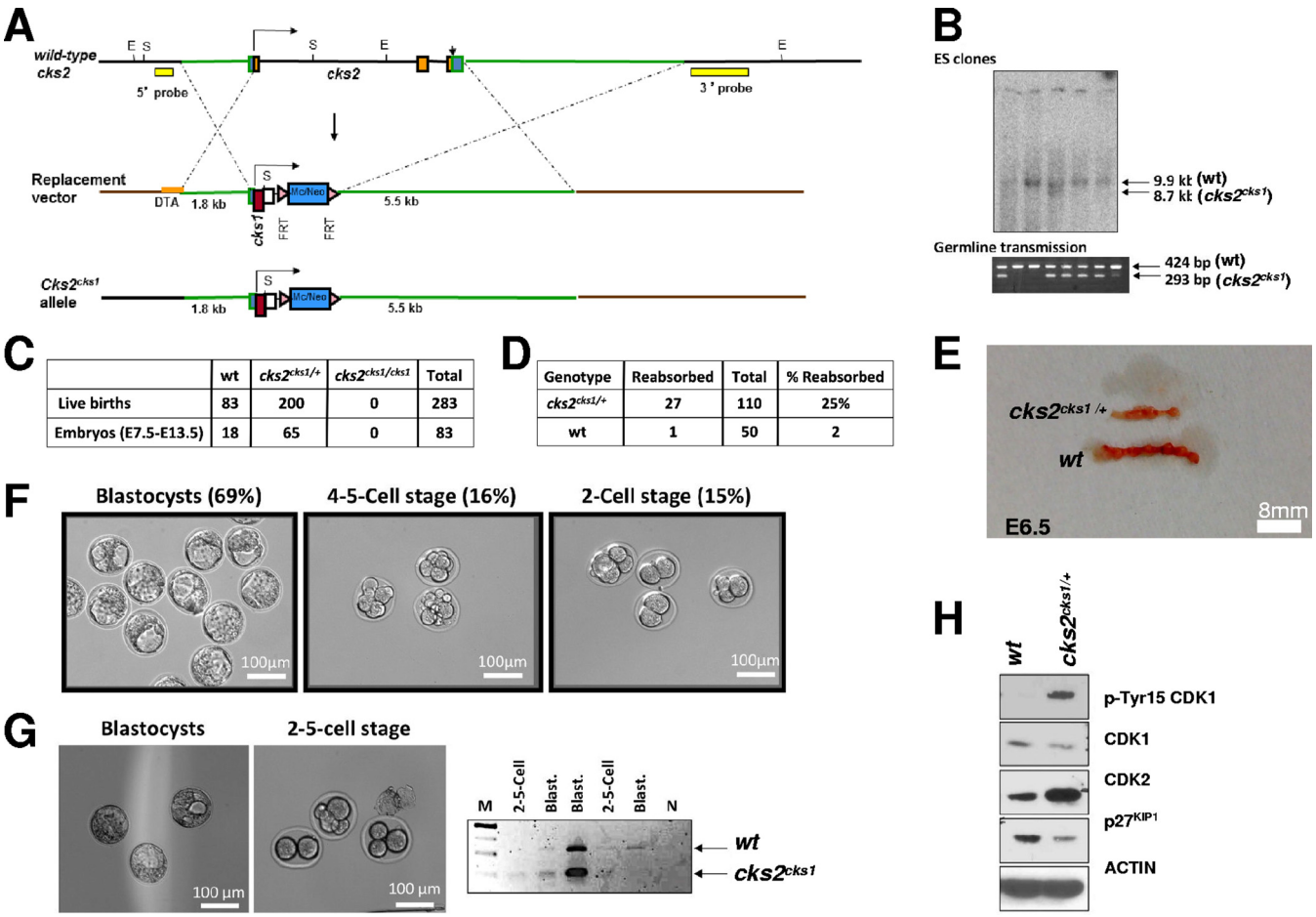

	wt	$cks2^{cks1/+}$	$cks2^{cks1/cks1}$	Total
Live births	83	200	0	283
Embryos (E7.5-E13.5)	18	65	0	83

Genotype	Reabsorbed	Total	% Reabsorbed
$cks2^{cks1/+}$	27	110	25%
wt	1	50	2

FIG 5 $cks2^{cks1/cks1}$ knock-in mice arrest embryonic development at the 2- to 5-cell stage. (A) Schematic showing the homologous recombination targeting strategy used to generate $cks2^{cks1/cks1}$ knock-in mice. (B) Genetic screening of ES cell clones for proper homologous recombination events by Southern blotting (top) and germ line transmission of the $cks2^{cks1}$ allele by PCR (bottom). (C) Genotyping results for adult progeny and E7.5 to E13.5 embryos from $cks2^{cks1/+}$ intercrosses showing the absence of homozygous mice and embryos. (D) Comparison of absorbed embryos from wt and $cks2^{cks1/+}$ intercrosses at E6.5. (E) Image showing absorbed embryos at E6.5 from $cks2^{cks1/+}$ intercrosses. (F) $cks2^{cks1/+}$ intercrosses produce a prevalence of embryos arrested at the 2-cell (15%) and 4- or 5-cell (16%) stages. (G) Images of blastocysts and 2- to 5-cell embryos (left) and representative PCR genotyping showing that the 2- to 5-cell-stage embryos from $cks2^{cks1/+}$ intercrosses are $cks2^{cks1/cks1}$. Lane M, molecular weight markers; lane N, no DNA. (H) Immunoblots showing reduced CDK1, increased p-Tyr15 CDK1, increased CDK2, and reduced $p27^{KIP1}$ in $cks2^{cks1/+}$ MEFs.

in mammalian meiosis, its expression in the germ line is deleterious for early embryonic development.

DISCUSSION

Delayed GVBD in $cks2^{-/-}$ oocytes. MPF regulates various cellular and molecular events during meiotic maturation, including GVBD, APC/C-mediated degradation of cyclin B1 and securin, polar body extrusion, and spindle assembly (22, 23). CKS proteins are a component of MPF, but their precise role(s) in regulating MPF functions during meiosis had not been fully delineated. Previously, it was shown that $cks2^{-/-}$ oocytes arrest maturation at metaphase of meiosis division I (15). In the present study, we extended these observations and now show that $cks2^{-/-}$ oocytes exhibit delayed GVBD. In mouse oocytes, GVBD is promoted by a surge in MPF-associated kinase activity that plateaus as oocytes approach metaphase of MI (24, 25). Consistent with the observed delay in GVBD, we found that MPF-associated kinase activity was delayed and reduced at all time points in $cks2^{-/-}$ oocytes following meiotic resumption. A similar delay was also observed for MAPK-associated kinase activity, which is stimulated by MPF (17). However, we found that microinjection of active MPF into $cks2^{-/-}$ oocytes could not completely rescue the GVBD delay, though the delay was rescued by MPF

plus CKS2. These data suggest that both CKS2's promotion of MPF component expression and MPF activity/substrate targeting are required for GVBD in mammalian oocytes.

It has been reported that deletion of CDK1 promotes the permanent arrest of oocytes at the GV stage, indicating that CDK1 is the sole CDK that is required and sufficient for the resumption of meiosis in mouse oocytes (24). Moreover, microinjection of CDK1 into *cdk1*$^{-/-}$ oocytes leads to progression and arrest in metaphase I (26). Our finding that GVBD is delayed in *cks2*$^{-/-}$ oocytes suggests that the absence of CKS2 could compromise CDK1 functions, possibly altering MPF's ability to target substrates whose phosphorylation promotes GVBD. The substrates of MPF-CKS2 that promote GVBD in mammalian oocytes are currently not known.

Defects in MPF expression in *cks2*$^{-/-}$ germ and somatic cells. During meiotic maturation, cellular events are ordered in a timely manner, which is regulated by the level of cyclin B (27). Previously, it was shown in budding yeast that CKS plays a direct role in transcriptional regulation by promoting the recruitment of CDK1 and the proteasome to coding regions (28). In mammalian cells, depletion of CKS1 and CKS2 impairs the transcription of *ccnb1*, *ccna2*, and *cdk1* (16). CKS2 was shown to associate with the promoters and open reading frames (ORFs) of these genes in G_2-phase cells, possibly contributing to their transcriptional activation, though the precise mechanism of action has not been delineated. We found that the levels of *ccna1*, *ccnb1*, *cdc20*, *cdk1*, and *cdk2* mRNAs were all downregulated in *cks2*$^{-/-}$ oocytes. Interestingly, the corresponding genes that encode these mRNAs harbor cell cycle-dependent element and cell cycle gene homology regions (CDE/CHR)-repressive promoter elements, which allow for expression in G_2-M phase of the cell division cycle (29). Our finding that *cks2*$^{-/-}$ oocytes, spermatocytes, and MEFs all contain reduced levels of *cdk1* mRNA suggests that CKS2 is an important transcriptional regulator of *cdk1* in germ and somatic cells. It will be of interest to determine whether CKS2 associates with the promoters of these genes during oocyte and spermatocyte maturation and whether CDE/CHR promoter elements play a role in regulating gene expression during meiosis.

CKS1 can compensate for CKS2 in meiosis *in vitro*. CKS1 and CKS2 have been shown to have both redundant and specialized roles in cell division control. For example, both CKS1 and CKS2 can bind CDK1 in human somatic cells (4). Additionally, the viability of *cks1*$^{-/-}$ and *cks2*$^{-/-}$ mice demonstrates that either CKS homolog can drive mitotic cell division cycles and development (13, 15). However, CKS1 accumulates in G_1/S phase and CKS2 accumulates in G_2/M phase in human cells, suggesting differential functions. One specialized function of CKS1 that has been identified is its role as an essential cofactor of the SCF^{SKP2} ubiquitin ligase, which mediates the degradation of several CDK2 inhibitors at the G_1/S phase transition. Since CKS2 is the only CKS paralog expressed in mouse oocytes and spermatocytes, it is suggested that CKS2 performs a specialized role in regulating CDK functions in mammalian meiosis (15), though previously it was shown that microinjection of *cks1* mRNA into *cks2*$^{-/-}$ oocytes could rescue the metaphase I arrest (15). In the current study, we also found that microinjection of CKS1 into prophase-arrested germinal vesicle (GV) stage *cks2*$^{-/-}$ oocytes promoted GVBD. Collectively, these results demonstrate that although CKS1 is excluded from the germ line, it can compensate for CKS2 functions in meiotic progression *in vitro*.

CKS1 is deleterious for early mammalian development. The exclusion of CKS1 from the mouse germ line is perplexing since CKS1 rescues the GVBD delay and metaphase I arrest in *cks2*$^{-/-}$ oocytes. Analysis of *cks2*$^{cks1/cks1}$ mice showed that CKS1 could compensate for CKS2 in meiosis *in vivo*, since *cks2*^{cks1} oocytes were generated and could be fertilized. However, homozygous *cks2*$^{cks1/cks1}$ embryos arrested development at the 2- to 5-cell stage, indicating that although CKS1 can compensate for CKS2 function in meiosis, its expression in the germ line and early embryonic cell division cycles is deleterious for development. The fact that both *cks1*$^{-/-}$ and *cks2*$^{-/-}$ mice are viable indicates that the premature expression of CKS1 in *cks2*$^{cks1/cks1}$ germ cells and embryos is likely responsible for the observed developmental arrest.

At the molecular level, the arrest of *cks2*$^{cks1/cks1}$ embryos at the 2- to 5-cell stage could be caused by CKS1 blocking the activation of MPF in early cell division cycles. In *Xenopus*, the CKS homolog Xe-p9 promotes CDK1-dependent phosphorylations of CDC25, MYT1, and WEE1, which in turn promote MPF activation (10). It is possible that CKS1 expressed from the *cks2* promoter, which displays differential strength and cell cycle regulation, could block these phosphorylations, leading to defective CDK1 activation. In support of this, we observed significantly increased pThr15-CDK1 in *cks2*$^{cks1/+}$ MEFs. Alternatively, CKS1 could interfere with the phosphorylation of a substrate(s) that is required for early embryonic cell division cycles that are normally mediated by MPF or MPF-CKS2. Another possibility is that the expression of CKS1 in the germ line promotes the premature activation of CDK2 and initiation of somatic cell division cycles, as was previously suggested (30). *cdk2*$^{-/-}$ mice of both sexes are sterile, with oocytes failing to transition from the pachytene to diplotene stage of prophase I (31, 32). In contrast, oocyte-specific deletion of *cdk2* from the primordial follicle stage showed that CDK2 is not required for oocyte maturation and female fertility (24). These results suggest that CDK2 is dispensable for meiotic resumption of GV stage oocytes. Very little is known regarding the precise functions of CDK2 in the transition from meiotic to somatic cell division cycles. We found that *cks2*$^{cks1/+}$ MEFs contained significantly reduced levels of p27^{KIP1}, a CDK2 inhibitor whose degradation is dependent on CDK2 activity and the SCF$^{SKP2\text{-}CKS1}$ ubiquitin ligase (13, 14). These data suggest that *cks1* expressed from the *cks2* promoter could drive the degradation of CDK2 inhibitors, resulting in the premature activation of CDK2-associated kinase activity. CKS1 could also promote the premature paralog-specific phosphorylation of CDK2 substrates during meiosis or early embryonic cell cycles, leading to the observed developmental arrest. Further studies will be needed to determine if the developmental arrest of *cks2*$^{cks1/cks1}$ embryos is CDK2 dependent and, if so, what substrates are prematurely targeted by CDK2-CKS1.

In summary, our study shows that CKS2 is a crucial regulator of MPF activity during meiosis and that its deletion in oocytes results in delayed MPF activation and GVBD and defective spindle assembly. Furthermore, *cks2*$^{cks1/cks1}$ knock-in mice revealed that CKS1 could compensate for CKS2 in mammalian meiosis *in vivo* but that its expression in the germ line is deleterious for early embryonic development.

MATERIALS AND METHODS

Oocyte collection, culture, and microinjection. All animal work was conducted according to Act No. 246/1992 of the Czech Republic for the protection of animals against cruelty. All institutional and national guidelines for the care and use of laboratory animals were followed accordingly. Oocytes were obtained from 8- to 12-week-old *cks2*$^{-/-}$ and wt female mice after injection of 5 IU of pregnant mare serum gonadotropin 43 to 48 h prior to scarification by cervical dislocation. Oocytes were collected in preheated M2 medium supplemented with 2.5 μM milrinone (Sigma-Aldrich) or 100 nM 3-isobutyl-1-methyl-xanthine (IBMX; Sigma-Aldrich) to prevent meiotic maturation, denuded by pipetting, washed, and cultured in M16 medium (Sigma-Aldrich) supplemented with 0.22 mM sodium pyruvate, 4-mg/ml bovine serum albumin (BSA; Sigma-Aldrich), and 1% penicillin-streptomycin (Sigma-Aldrich) at 37°C in a 5% CO_2 atmosphere. After an IBMX-milirinone wash, at least 90% of oocytes resumed meiosis (GVBD) within 70 min.

GV stage oocytes were microinjected in transfer medium (34) with IBMX on an inverted Leica DMI 6000B microscope with a Transferman NK2 micromanipulator and a FemtoJet microinjector (Eppendorf). Approximately 5 pl of a solution of active CDK1-cyclin B1 cocktail (catalog number SRP5009; Sigma) and/or recombinant proteins diluted in RNase-free water was microinjected. The inactivated MPF cocktail was obtained by denaturation at 95°C for 5 min.

Spermatocyte isolation and separation. A pool of spermatogenic cells was isolated from the testes of mice. Testes were decapsulated and transferred to 20 ml of testis isolation medium (TIM; 0.1 M NaCl, 0.05 M KCl, 1.2 mM $CaCl_2$, 1.2 mM $MgSO_4$, 6 mM Na_2HPO_4, 0.7 mM KH_2PO_4, 0.1% glucose, 0.04% L-glutamine, 1 mM sodium pyruvate, 6 mM sodium-DL-lactate, antibiotics). The seminiferous tubules were dispersed by incubation with 2-mg/ml collagenase, followed by 0.35-mg/ml trypsin, and the reaction was stopped by addition of 1% BSA. Pachytene spermatocytes were separated by velocity sedimentation with a Sta-Put cell separator. Different cell types were sedimented through a linear BSA gradient according to their cell size. Pachytene spermatocytes were collected and optionally cultured in medium with 2 to 5 μM ocadaic acid (Sigma-Aldrich) for 2 h to induce meiotic maturation.

Kinase assays. CDK1 and mitogen-activated protein (MAP) kinase activities were measured by their capability to phosphorylate the external substrates histone H1 and MBP, respectively (33). Ten oocytes per sample were collected at the indicated times and lysed in 5 μl of homogenization buffer (40 mM

MOPS [morpholinepropanesulfonic acid; pH 7.2], 20 mM NaF, 20 mM *para*-nitrophenyl phosphate, 40 mM β-glycerophosphate, 0.2 mM Na_3VO_4, 10 mM EGTA, 0.2 mM EDTA, 2 mM benzamidine, 20 μg/ml leupeptin, 20 μg/ml aprotinin, 1 mM phenylmethylsulfonyl fluoride) by three to five cycles of freezing-thawing in liquid nitrogen. Next, 2.5 μl of 4$\times$ kinase buffer (50 mM MOPS [pH 7.2], 10 mM $MgCl_2$, 5 mM EGTA, 0.1 mM EDTA, 1 mM dithiothreitol, 0.4 μM protein kinase C inhibitor 1, a cocktail of phosphatases and protease inhibitors) containing 10 mg/ml histone H1 and 5 mg/ml MBP was mixed with 1.5 μl of 0.1 mM ATP and 1 μl of 10-mCi/ml [γ-^{32}P]ATP (Amersham Pharmacia Biotech), and the mixture was incubated with the lysed sample for 30 min at 37°C. Reactions were terminated by the addition of SDS-PAGE loading buffer and incubation at 95°C for 5 min. Samples were then run on 12% SDS-PAGE gels, dried, and subjected to autoradiography.

qRT-PCR analysis. RNA was isolated from mouse oocytes by adding 10 μl of lysis buffer and 1 μl of enhancer, and the mixture was incubated for 10 min at 75°C, followed by DNase treatment for 10 min at room temperature. RNA from MEFs and spermatocytes was isolated using an RNeasy Plus minikit (Qiagen). qRT-PCRs were performed using standard techniques. Primers were designed on the intron borders to eliminate potential DNA amplifications. The sequences of the primers used were as follows: for *cdk1*, 5′-CTCGGCTCGTTACTCCACTC-3′ and 5′-ACTCGACTTCTGGCCACACT-3′; for *ccnb1*, 5′-CTTGGAG AGGGATTATCA-3′ and 5′-ACCAGAGGTGGAACTTGCTG-3′; for *ccna1*, 5′-GTGGTGATTCAAAACTGCCA-3′ and 5′-GGCCAGCTGAGCTTAAAGAA-3′; for *cdk2*, 5′-GAAATTCTTCTGGGCTGCAA-3′ and 5′-CGAAAGATCC GGAAGAGTTG-3′; for *e2f1*, 5′-CAGCATGTTGTCAGTGGCTT-3′ and 5′-GGGATCGCAGAGACCATAGA-3′; for *bmyb*, 5′-TCTGGATGAGTTACACTACCAGG-3′ and 5′-GTGCGGTTAGGAAAGTGACTG-3′; for *cdc20*, 5′-CTGG AGGTGACCGCTTTATCC-3′ and 5′-TCAAAACCGTTCAGGTTGAGAGA-3′; and for *gapdh*, 5′-TTGAGGTCAAT GAAGGGGTC-3′ and 5′-TCGTCCCGTAGACAAAATGG-3′.

Immunocytochemistry (ICC). Oocytes were fixed in 4% paraformaldehyde (PFA) in phsopahte-buffered saline (PBS) for 30 min, permeabilized for 15 min in PBS with 0.1% Triton X-100, and incubated overnight at 4°C with primary antibodies (1:100) against p-CDC27 (catalog number ab12281; Abcam), securin, acetylated tubulin (catalog number T6793; Sigma-Aldrich), Crest antibody (Thermo Fisher), and lamin A/C (catalog number SAB4200236; Sigma-Aldrich). Cortical actin was visualized by actin-green phalloidin 488 (Thermo Fisher). After washing, the oocytes were incubated for 1 h at room temperature with Alexa Fluor-conjugated antibodies (1:250; Molecular Probes). DAPI (4′,6-diamidino-2-phenylindole) was used for chromosome staining (Vectashield). Samples were visualized using an inverted confocal microscope in 16-bit depth (TCS SP5; Leica). Images were assembled in Photoshop CS3 software.

Live cell imaging. At 1 to 2 h postmicroinjection, oocytes were washed in transfer medium and transferred in M16 medium to a Leica AF6000 wide-field automated microscope equipped with a conditioned chamber of 37°C and 5% CO_2 atmosphere. Time-lapse imaging was performed for 16 h using Leica LAS AF software. Progression of meiotic maturation was analyzed manually.

MEF isolation and retroviral infections. MEFs (wt, *cks2*$^{-/-}$, *cks2*$^{cks1/+}$) were derived by incubating E13.5 embryos, devoid of internal organs or head, in 0.5% trypsin for 3 h at 37°C and then seeding the cells in Dulbecco modified Eagle medium supplemented with 10% fetal bovine seurm. At least 3 embryos of the same genotype were pooled, and cells were passaged for 2 or 3 population doublings before the described experiments were performed. MEFs were infected with retroviruses (pBABE) that express Flag-*cks2* using standard techniques.

SDS-PAGE and Western blot analysis. Cells were lysed in radioimmunoprecipitation assay (RIPA) buffer (150 mM NaCl, 5 mM EDTA, 0.05% NP-40, 1% sodium deoxycholate, 0.1% SDS, 1% Triton X-100, and 50 mM Tris-HCl [pH 7.4] with phosphatase and protease inhibitors), sonicated, and centrifuged at 10,000 $\times$ *g* for 10 min at 4°C. Samples were adjusted to the total number of oocytes or total protein (10 μg of total protein per sample) and loaded onto 12% or 15% Tris-acetate gels. Gels were transferred onto polyvinylidene difluoride membranes, blocked in 5% skimmed milk in 1$\times$ Tris-buffered saline with Tween 20 (TBST), and probed overnight at 4°C with antibody diluted in 5% milk in 1$\times$ TBST. The following antibodies were used: anti-phosphorylated Tyr15 CDK1 (catalog number cs-4539; Cell Signaling), anti-CDK1 (catalog number sc-8395; Santa Cruz Biotechnology), anti-CDK2 (catalog number sc-6248; Santa Cruz Biotechnology), anti-p27^{KIP1} (catalog number 610241; BD Biosciences), antiactin (catalog number sc-58673; Santa Cruz Biotechnology), anti-phosphorylated p44/42 MAPK (Thr202/Tyr204; catalog number cs-9101; Cell Signaling), and anti-p44/42 MAPK (catalog number cs-9102; Cell Signaling). Secondary antibodies conjugated with horseradish peroxidase (anti-mouse immunoglobulin [catalog number 711-035-152; Jackson ImmunoResearch] or anti-rabbit immunoglobulin [catalog number 711-035-152; Jackson ImmunoResearch]) were used. The signals were revealed by chemiluminiscence (ECL; catalog number 28980926; APCzech).

Generation of *cks2*^{cks1} knock-in mice. A *cks2*^{cks1} replacement vector based on the vector pBKSII-FRT-mc/Neo was constructed. DNA fragments of 1.8 kb and 5.5 kb in length corresponding to sequences immediately upstream and downstream of the mouse *cks2* coding region, respectively, were amplified using a high-fidelity polymerase, verified by DNA sequencing, and subcloned into the cloning sites flanking the FRT-mc/Neo-FRT cassette. *cks1* cDNA containing a stop codon was then cloned into the vector, such that proper homologous recombination would result in *cks1* expression under the control of the *cks2* promoter, with the appropriate upstream and 3′ untranslated region sequences. A *pgk-dta* cassette was included for negative selection. The *cks2*^{cks1} knock-in vector was then electroporated into 129/SvJ mouse embryonic stem (ES) cells, and neomycin-resistant (Neo^r) clones were isolated. Positive ES cell clones were identified by Southern blotting and then subsequently injected into C57BL/6J mouse blastocysts to generate chimeric mice. Germ line transmission of the *cks2*^{cks1} allele was followed by PCR. The Mc/Neo cassette was then excised by crossing *cks2*$^{cks1/+}$ mice with *frt*-expressing transgenic mice.

Southern blotting and genotyping. Southern blot analysis was performed using an 1,138-bp probe corresponding to a DNA sequence adjacent to the *cks2* mouse locus that was amplified with primers 5′-ACTCTGCTCATGACCCACCT-3′ and 5′-TTTGGTTTTCAAATGCACCA-3′. DNA from Neo^r ES clones was cut with EcoRI. A 9.9-kb band was predicted for the wt allele, and a 8.7-kb band indicated proper homologous recombination. PCR-based genotyping of adult mice and embryos was performed using a multiplexed PCR with primers 5′-GCAACAGGCTTCTGATTGGT-3′, 5′-ACATGACATGCCGGTATTCG-3′, and 5′-TAACGACTCCCCATCTCCTG-3′. A 293-bp product corresponded to the *cks2*^{cks1} allele, and a 424-bp product corresponded to the wt *cks2* allele. Deletion of the FLP recombination target (FRT) cassette was determined by inclusion of primer 5′-ACGAATGTGGCACCTGAACT-3′. DNA was isolated from blastocysts and early embryos by adding 5 μl of 10 mM Tris and 5 mM EDTA and boiling for 3 min. Proteinase K (1 μl of a 1-μg/μl solution) was added, and the mixture was incubated overnight at 56°C and then heat inactivated. DNA (5 μl) was then genotyped using a nested PCR protocol with external primers 5′-GAG CAATTCATCCACTGCAA-3′ and 5′-TCAACAATGGTGATATAAATGCAA-3′ and internal primers 5′-TGATCCC GCTTACTCCTCTG, 5′-ATCCCTGACTCTGCTGAACG-3′, and 5′-CCATCTAACGACTCCCCATC-3′. The *cks2*^{cks1} allele corresponded to a 198-bp PCR product, and the wt *cks2* allele corresponded to a 333-bp product.

Embryo/blastocyst isolations. Two-month-old female *cks2*$^{cks1/+}$ mice from the same litter were injected with 5 IU of pregnant mare serum gonadotropin and 5 IU of human chorionic gonadotropin (hCG) 43 to 48 h prior to mating with males. The next morning, females positive for vaginal plugs were separated. Mice were sacrificed at E3.5 for blastocyst isolations and E7.5 or later for embryo isolations. Blastocysts were then flushed from oviducts with preheated M2 medium (Sigma-Aldrich), photographed, and subsequently used for genotyping or ICC analysis.

Statistical analysis. All experiments were repeated at least three times unless otherwise indicated. Mean and standard deviation (SD) values were calculated using MS Excel software, and statistical significance was tested using Student's *t* test (GraphPad Prism [version 5] software), with a *P* value of <0.05 being considered statistically significant.

ACKNOWLEDGMENTS

We thank Silvia Evans (University of California at San Diego) for plasmid pBKSII-FRT-mc/Neo and FRT-expressing transgenic mice. We thank Jaroslava Supolikova, Marketa Hancova, and Marie Valova for their exceptional assistance with experiments.

This work was supported by NIH/NICHD grant 7RO1HD049539 to C.S. and by the National Sustainability Program project number LO1609 (Czech Ministry of Education, Youth and Sports), GACR15-22765S, 18-19395S Excellence CZ.02.1.01/0.0/0.0/15_003/0000460 OP RDE, and Institutional Research Concept RVO67985904.

REFERENCES

1. Hayles J, Beach D, Durkacz B, Nurse P. 1986. The fission yeast cell cycle control gene cdc2: isolation of a sequence suc1 that suppresses cdc2 mutant function. Mol Gen Genet 202:291–293. https://doi.org/10.1007/BF00331653.
2. Hadwiger JA, Wittenberg C, Mendenhall MD, Reed SI. 1989. The Saccharomyces cerevisiae CKS1 gene, a homolog of the Schizosaccharomyces pombe suc1$^+$ gene, encodes a subunit of the Cdc28 protein kinase complex. Mol Cell Biol 9:2034–2041. https://doi.org/10.1128/MCB.9.5.2034.
3. Reed SI, Hadwiger JA, Richardson HE, Wittenberg C. 1989. Analysis of the Cdc28 protein kinase complex by dosage suppression. J Cell Sci Suppl 12:29–37.
4. Richardson HE, Stueland CS, Thomas J, Russell P, Reed SI. 1990. Human cDNAs encoding homologs of the small p34Cdc28/Cdc2-associated protein of Saccharomyces cerevisiae and Schizosaccharomyces pombe. Genes Dev 4:1332–1344. https://doi.org/10.1101/gad.4.8.1332.
5. Tang Y, Reed SI. 1993. The Cdk-associated protein Cks1 functions both in G1 and G2 in Saccharomyces cerevisiae. Genes Dev 7:822–832. https://doi.org/10.1101/gad.7.5.822.
6. Reynard GJ, Reynolds W, Verma R, Deshaies RJ. 2000. Cks1 is required for G(1) cyclin-cyclin-dependent kinase activity in budding yeast. Mol Cell Biol 20:5858–5864. https://doi.org/10.1128/MCB.20.16.5858-5864.2000.
7. Moreno S, Hayles J, Nurse P. 1989. Regulation of p34cdc2 protein kinase during mitosis. Cell 58:361–372. https://doi.org/10.1016/0092-8674(89)90850-7.
8. Patra D, Dunphy WG. 1996. Xe-p9, a Xenopus Suc1/Cks homolog, has multiple essential roles in cell cycle control. Genes Dev 10:1503–1515. https://doi.org/10.1101/gad.10.12.1503.
9. Bourne Y, Watson MH, Hickey MJ, Holmes W, Rocque W, Reed SI, Tainer JA. 1996. Crystal structure and mutational analysis of the human CDK2 kinase complex with cell cycle-regulatory protein CksHs1. Cell 84:863–874. https://doi.org/10.1016/S0092-8674(00)81065-X.
10. Patra D, Wang SX, Kumagai A, Dunphy WG. 1999. The Xenopus Suc1/Cks protein promotes the phosphorylation of G(2)/M regulators. J Biol Chem 274:36839–36842. https://doi.org/10.1074/jbc.274.52.36839.
11. Patra D, Dunphy WG. 1998. Xe-p9, a Xenopus Suc1/Cks protein, is essential for the Cdc2-dependent phosphorylation of the anaphase-promoting complex at mitosis. Genes Dev 12:2549–2559. https://doi.org/10.1101/gad.12.16.2549.
12. Morris MC, Kaiser P, Rudyak S, Baskerville C, Watson MH, Reed SI. 2003. Cks1-dependent proteasome recruitment and activation of CDC20 transcription in budding yeast. Nature 423:1009–1013. https://doi.org/10.1038/nature01720.
13. Spruck C, Strohmaier H, Watson M, Smith AP, Ryan A, Krek TW, Reed SI. 2001. A CDK-independent function of mammalian Cks1: targeting of SCF(Skp2) to the CDK inhibitor p27Kip1. Mol Cell 7:639–650. https://doi.org/10.1016/S1097-2765(01)00210-6.
14. Ganoth D, Bornstein G, Ko TK, Larsen B, Tyers M, Pagano M, Hershko A. 2001. The cell-cycle regulatory protein Cks1 is required for SCF(Skp2)-mediated ubiquitinylation of p27. Nat Cell Biol 3:321–324. https://doi.org/10.1038/35060126.
15. Spruck CH, de Miguel MP, Smith APL, Ryan A, Stein P, Schultz RM, Lincoln AJ, Donovan PJ, Reed SI. 2003. Requirement of Cks2 for the first metaphase/anaphase transition of mammalian meiosis. Science 300:647–650. https://doi.org/10.1126/science.1084149.
16. Martinsson-Ahlzen H-S, Liberal V, Grunenfelder B, Chaves SR, Spruck CH, Reed SI. 2008. Cyclin-dependent kinase-associated proteins Cks1 and Cks2 are essential during early embryogenesis and for cell cycle progression in somatic cells. Mol Cell Biol 28:5698–5709. https://doi.org/10.1128/MCB.01833-07.
17. Minshull J, Sun H, Tonks NK, Murray AW. 1994. A MAP kinase-dependent spindle assembly checkpoint in Xenopus egg extracts. Cell 79:475–486. https://doi.org/10.1016/0092-8674(94)90256-9.

18. Kotani S, Tanaka H, Yasuda H, Todokoro K. 1999. Regulation of APC activity by phosphorylation and regulatory factors. J Cell Biol 146: 791–800. https://doi.org/10.1083/jcb.146.4.791.
19. Huang J-Y, Morley G, Li D, Whitaker M. 2007. Cdk1 phosphorylation sites on Cdc27 are required for correct chromosomal localisation and APC/C function in syncytial Drosophila embryos. J Cell Sci 120:1990–1997. https://doi.org/10.1242/jcs.006833.
20. Brunet S, Pahlavan G, Taylor S, Maro B. 2003. Functionality of the spindle checkpoint during the first meiotic division of mammalian oocytes. Reproduction 126:443–450. https://doi.org/10.1530/rep.0.1260443.
21. Curtis D, Lehmann R, Zamore PD. 1995. Translational regulation in development. Cell 81:171–178. https://doi.org/10.1016/0092-8674(95)90325-9.
22. Choi T, Aoki F, Mori M, Yamashita M, Nagahama Y, Kohmoto K. 1991. Activation of p34cdc2 protein kinase activity in meiotic and mitotic cell cycles in mouse oocytes and embryos. Development 113:789–795.
23. Verlhac MH, Kubiak JZ, Clarke HJ, Maro B. 1994. Microtubule and chromatin behavior follow MAP kinase activity but not MPF activity during meiosis in mouse oocytes. Development 120:1017–1025.
24. Adhikari D, Zheng W, Shen Y, Gorre N, Ning Y, Halet G, Kaldis P, Liu K. 2012. Cdk1, but not Cdk2, is the sole Cdk that is essential and sufficient to drive resumption of meiosis in mouse oocytes. Hum Mol Genet 21:2476–2484. https://doi.org/10.1093/hmg/dds061.
25. Adhikari D, Liu K. 2014. The regulation of maturation promoting factor during prophase I arrest and meiotic entry in mammalian oocytes. Mol Cell Endocrinol 382:480–487. https://doi.org/10.1016/j.mce.2013.07.027.
26. Santamaría D, Barrière C, Cerqueira A, Hunt S, Tardy C, Newton K, Cáceres JF, Dubus P, Malumbres M, Barbacid M. 2007. Cdk1 is sufficient to drive the mammalian cell cycle. Nature 448:811–815. https://doi.org/10.1038/nature06046.
27. Polanski Z, Ledan E, Brunet S, Louvet S, Verlhac MH, Kubiak JZ, Maro B. 1998. Cyclin synthesis controls the progression of meiotic maturation in mouse oocytes. Development 125:4989–4997.
28. Yu V, Baskerville C, Grünenfelder B, Reed SI. 2005. A kinase-independent function of Cks1 and Cdk1 in regulation of transcription. Mol Cell 17:145–151. https://doi.org/10.1016/j.molcel.2004.11.020.
29. Müller GA, Engeland K. 2010. The central role of CDE/CHR promoter elements in the regulation of cell cycle-dependent gene transcription. FEBS J 277:877–893. https://doi.org/10.1111/j.1742-4658.2009.07508.x.
30. Donovan PJ, Reed SI. 2003. Germline exclusion of Cks1 in the mouse reveals a metaphase I role for Cks proteins in male and female meiosis. Cell Cycle 2:275–276.
31. Berthet C, Aleem E, Coppola V, Tessarollo L, Kaldis P. 2003. Cdk2 knockout mice are viable. Curr Biol 13:1775–1785. https://doi.org/10.1016/j.cub.2003.09.024.
32. Ortega S, Prieto I, Odajima J, Martín A, Dubus P, Sotillo R, Barbero JL, Malumbres M, Barbacid M. 2003. Cyclin-dependent kinase 2 is essential for meiosis but not for mitotic cell division in mice. Nat Genet 35:25–31. https://doi.org/10.1038/ng1232.
33. Motlík J, Sutovský P, Kalous J, Kubelka M, Moos J, Schultz RM. 1996. Co-culture with pig membrana granulosa cells modulates the activity of cdc2 and MAP kinase in maturing cattle oocytes. Zygote 4:247–256. https://doi.org/10.1017/S0967199400003166.
34. Tetkova A, Hancova M. 2016. Mouse oocyte isolation, cultivation and RNA microinjection. Bio-protocol 6(3):e1729. https://doi.org/10.21769/BioProtoc.1729.